

# Gravitational Deflection of Vector Photons via Effective Field Theory

---

**Yihan Ma & Ding-fang Zeng**

*School of Physics and Optoelectronic Engineering, Beijing University of Technology*

*E-mail: [yihan.ma@emails.bjut.edu.cn](mailto:yihan.ma@emails.bjut.edu.cn), [dfzeng@bjut.edu.cn](mailto:dfzeng@bjut.edu.cn)*

**ABSTRACT:** We calculate the gravitational scattering amplitude of an electromagnetic field off a heavy scalar field with the effective field theory method. From this we derive the photon deflection angle caused by massive bodies in the weak field approximation. Our calculation focuses on the long-range interaction exclusively, which is determined by the non-analytic terms of the momentum transfer in the amplitude. Using geometric optics and eikonal approximations, we derive expressions for the deflection angle. In contrast to previous works, we utilise the integration-by-parts reduction technique to the one-loop amplitudes, avoiding direct computations of a large number of Feynman integrals. Our calculation is performed in the covariant Lorenz gauge and harmonic coordinate condition. It includes contributions from the scalar and vector ghost fields to the scattering amplitude. Differences between our results and those in the literature are pointed out explicitly, and the origin is analysed briefly.

# Contents

<b>1</b>	<b>Introduction</b>	<b>1</b>
<b>2</b>	<b>The calculation of the scattering amplitude</b>	<b>3</b>
2.1	Scattering amplitude at tree-level	4
2.2	Scattering amplitude at one-loop level	5
<b>3</b>	<b>The deflection angle of photon trajectory</b>	<b>9</b>
3.1	Geometric optics approximation	10
3.2	Eikonal approximation	11
3.3	Discussion on the result	13
<b>4</b>	<b>Conclusion</b>	<b>14</b>
	<b>Reference</b>	<b>15</b>

## 1 Introduction

The shadow image of the supermassive black holes in the center of M87 galaxy and our Milky Way taken by the Event Horizon Telescope Collaboration [1–4] gains tremendous sensation in the community. The theoretical basis of this achievement is closely related with the lensing formula derived by K.S. Virbhadra and G. F.R. Ellis, which describes the deflection angle of light rays passing through the gravitational field of a Schwarzschild black hole [5, 6]. Accurately calculating the gravitational lensing effects is the key to obtain clear image of black holes. This determines how well we can understand the black hole and its environment.

Based on the work of K.S. Virbhadra and G.F.R. Ellis, S. Frittelli et al. [7], V. Bozza et al. [8], and N. Tsukamoto [9] further refined the method to calculate the gravitational lensing effect in strong gravitational fields. As for the weak field regime, we have other alternative ways to calculate the deflection angle, such as impulse approximation and topological methods based on the Gauss–Bonnet theorem [6, 10]. Besides these methods, in recent years, Effective Field Theory (EFT) [11–13] is also introduced into the research of gravitational lensing effects, as a special case of the more general phenomena of gravitational scattering.

In conventional applications of this method, researchers derive the light deflection angle from the photon-black hole scattering amplitude [14–16]. However, the vertices of gravity-photon interaction and gravity-gravity self-interaction become more and more complex as the perturbation order increases. As a way out, the modern EFT method uses the KLT (Kawai-Lewellen-Tye) relation [17, 18], which expresses the gravitational scattering amplitudes as products of Yang-Mills amplitudes. Combined with the unitarity technique [19], this approach allows researchers to directly derive

the non-analytic terms in the momentum transfer at the one-loop level. These terms, after Fourier transformation, can be used to extract the long-range gravitational effective potential [20, 21], from which the deflection angle of photons is then routinely determined.

Another way to reduce the workload of EFT method is to adopt the modern loop integration techniques, such as the Integration-by-Parts (IBP) reduction. IBP reduction allows us to focus on very few master integrals instead of directly evaluating a vast number of Feynman integrals. A key advantage of this technique is its applicability to higher-loop calculations. In ref.[16], this method was utilized to calculate the deflection of scalar photon trajectories at the one-loop level. Here, we extend this approach to one-loop amplitudes for the more realistic scenario of vector-photon scattering off black holes. We will take a heavy scalar field as proxies for black holes. Most of the repetitive but routine tasks, such as the Feynman rules' generation and the Feynman integral's reduction, will be treated by computational tools. Several packages are available for the IBP reduction, such as FIRE6 and Kira (both are based on the Laporta algorithm [22]), and LiteRed [23, 24]. For this work, we choose LiteRed.

We will take a massive scalar field  $\phi$  to denote black holes, a standard vector field  $A$  to denote the photon and a second order tensor field  $h$  to denote the graviton, and write the effective action controlling the interaction between these objects as follows:

$$e^{iS_{\text{eff}}} = \int \mathcal{D}\phi \mathcal{D}A \mathcal{D}h \mathcal{D}\bar{c}_h \mathcal{D}c_h \mathcal{D}\bar{c}_A \mathcal{D}c_A e^{i(S_\phi + S_h + S_A + S_{\text{ghost}})}. \quad (1.1)$$

$c_A$  &  $c_h$  here are the ghost fields of the electromagnetic and gravitational fields, respectively.

$$S_\phi = \int d^4x \frac{\sqrt{-g}}{2} (\partial^\mu \phi \partial_\mu \phi - m^2 \phi^2), \quad (1.2)$$

$$S_h = \kappa^{-2} \int d^4x \sqrt{-g} (2R + \kappa^2 \mathcal{G}_h^\mu \mathcal{G}_{h\mu}), \quad (1.3)$$

$$S_A = \int d^4x \sqrt{-g} \left( -\frac{1}{4} F^{\mu\nu} F_{\mu\nu} + \frac{1}{2} \mathcal{G}_A^2 \right), \quad (1.4)$$

where  $\kappa = \sqrt{32\pi G_N}$ , (1.4),  $\mathcal{G}_h^\mu$ ,  $\mathcal{G}_A$  are the gauge-fixing factors of the gravitational and electromagnetic fields,

$$\mathcal{G}_h^\mu = \Gamma^\mu, \quad \mathcal{G}_A = D^\mu A_\mu. \quad (1.5)$$

With the help of xAct package[25–27], we can derive the desired Feynman rules from (1.2)-(1.4). We confirmed that they are consistent with the rules provided by B. Latosh in FeynGrav [28, 29].

The structure of our paper is as follows. In Section 2, we calculate the amplitude of photon & heavy-scalar-field scattering in the center-of-mass frame and present the

results in the small-angle approximation. In Section 3, we derive the deflection angle of photon trajectories passing through the gravitational field of massive objects using the Eikonal and geometric optic approximations, comparing our results with those in the existing literature. In Section 4, we summarize the calculational results of the paper.

## 2 The calculation of the scattering amplitude

We choose to calculate the tree-level and one-loop amplitude of the photon-black holes in the center of mass frame, as shown in Figure 1. We will take the direction of the ingoing photon's momentum as the direction of positive z-axis. So in the in-out formalism, the polarization vectors of the ingoing and outgoing photons are as follows,

$$\epsilon_i^{+\mu} = \frac{1}{\sqrt{2}}(0, 1, i, 0), \epsilon_i^{-\mu} = \frac{1}{\sqrt{2}}(0, 1, -i, 0), \quad (2.1)$$

$$\epsilon_o^{+\mu} = \frac{1}{\sqrt{2}}(0, \cos \theta, i, -\sin \theta), \epsilon_o^{-\mu} = \frac{1}{\sqrt{2}}(0, \cos \theta, -i, -\sin \theta). \quad (2.2)$$

The superscript “+” here denotes the right-handed polarization, while the “-” subscript denotes the left-handed polarization.

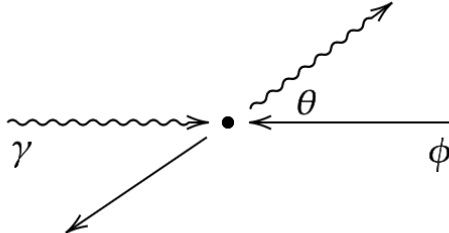


**Figure 1.** Diagram of  $\gamma - \phi$  scattering in the center-of-mass frame.

According to the on-shell condition of the external particles and the conservation of four momentum, we have

$$k_i^2 = k_o^2 = 0, \quad p_i^2 = p_o^2 = m^2, \quad (2.3)$$

$$k_i + p_i - k_o - p_o = 0, \quad (2.4)$$

where  $k_i$  &  $k_o$  represent the incoming and outgoing momentum of the photons,  $\omega$  is their energies;  $p_i$  &  $p_o$  represent the incoming and outgoing momentum of heavy scalar field, with  $m$  being its invariant mass. The Mandelstam variables of the scattering process are

$$s = (k_i + p_i)^2, \quad t = (k_i - k_o)^2, \quad u = (k_i - p_o)^2. \quad (2.5)$$

As usual, the three Mandelstam variables are related by the standard relation

$$s + t + u = 2m^2. \quad (2.6)$$

By these definition, we can easily show that in the low-energy regime, the following expressions hold,

$$s \simeq m^2 + 2m\omega, \quad t \simeq -\mathbf{q}^2, \quad u \simeq m^2 - 2m\omega + \mathbf{q}^2, \quad (2.7)$$

where  $q$  is a four-dimensional form of the transferred momentum, with  $\mathbf{q}$  being its three-dimensional components.

## 2.1 Scattering amplitude at tree-level

At the tree level, only the t-channel diagram contributes to the amplitude of photon-black hole scattering process, as shown in Figure 2, where  $q^\mu = k_o^\mu - k_i^\mu = (0, \mathbf{q})$  is the momentum transfer of the process.

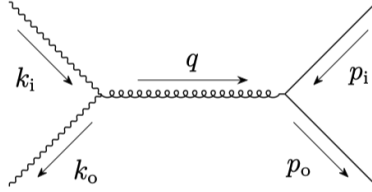


**Figure 2.** Tree-level Feynman diagram of t-channel

According to the Feynman rules derived from eq.(1.1), in the case the polarization states of the outgoing and incoming photons are the same, the scattering amplitude at the tree level can be written as

$$i\mathcal{M}^{(t)} = \epsilon_{i\mu}^+(\epsilon_{o\nu}^+)^* i\mathcal{M}^{(t)\mu\nu} \quad (2.8)$$

$$= \epsilon_{i\mu}^+(\epsilon_{o\nu}^+)^* \frac{V_{(AAh)}^{\mu\nu\mu_1\nu_1}[k_i, -k_o, -q] P_{\mu_1\nu_1\mu_2\nu_2}^{(g)} V_{BBh}^{\mu_2\nu_2}[p_i, -p_o]}{t} \quad (2.9)$$

$$= -i\kappa^2 m^2 \cos^2 \frac{\theta}{2} \left[ \frac{-2(2\zeta + 1)\zeta^2 \cos \theta + 2\xi\zeta + \xi + 2(2\zeta + 3)\zeta^2}{4\xi} \right]. \quad (2.10)$$

While in the case the polarization states of the outgoing and incoming photons are different, we have

$$\epsilon_{i\mu}^+(\epsilon_{o\nu}^-)^* \mathcal{M}^{\mu\nu}_t = i\kappa^2 m^2 \sin^2 \frac{\theta}{2} \left[ \frac{-2(2\zeta + 1)\zeta^2 \cos \theta + 2\xi\zeta + \xi + 2(1 - 2\zeta)\zeta^2}{4\xi} \right], \quad (2.11)$$

where  $\xi \equiv t/m^2$  and  $\zeta \equiv \omega/m$ . From eq.(2.11), we can see that at  $\mathcal{O}(\theta^0)$ , the polarization of the photon does not change during the scattering process.

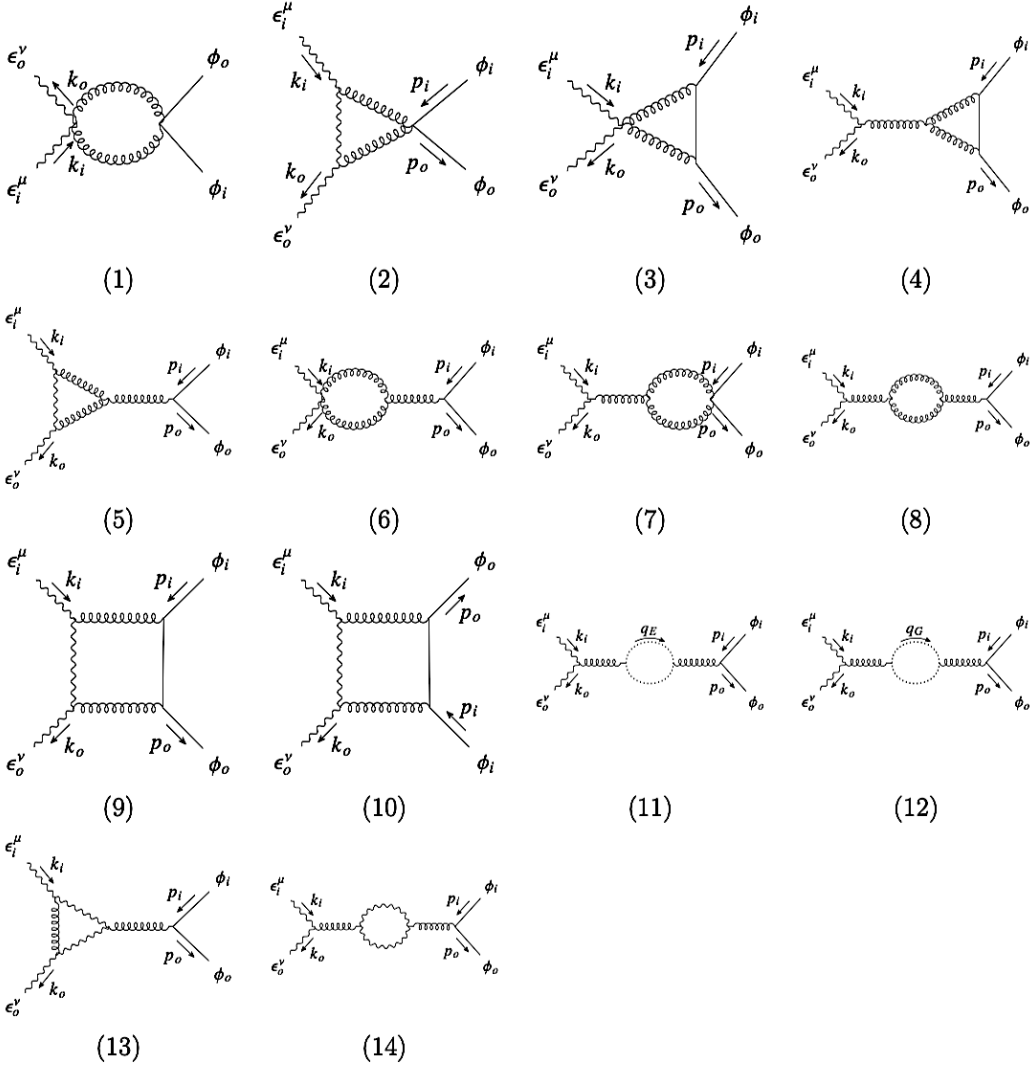


**Figure 3.** The one-loop Feynman graphs of the scattering of photon-heavy scalar field that needs to be calculated

## 2.2 Scattering amplitude at one-loop level

At the one-loop order, the Feynman diagrams need be calculated are shown in Figure 3, where  $q_E$  represents the ghost field which originates from the gauge fixing of the electromagnetic field,  $q_G$  denotes the ghost field arising from the gauge fixing of gravitational field. We will use the following notations to simplify expressions of the scattering amplitude,

$$\begin{aligned}
 D_1 &\equiv q^2, \quad D_2 \equiv (k_i - q)^2, \quad D_3 \equiv (k_i - k_o - q)^2, \\
 D_4 &\equiv (p_i + q)^2 - m^2, \quad D_5 \equiv (q - p_o)^2 - m^2.
 \end{aligned}
 \tag{2.12}$$

The first issue we encounter in the calculation of one-loop diagrams is the treatment of  $\epsilon_{i,o} \cdot q$  factors in the amplitude denoted by the the first Feynman digram in

Figure 3,

$$\epsilon_{i\mu}\epsilon_{o\nu}^* V_{AAhh}^{\mu\nu\mu_1\nu_1}[k_i, -k_o, -q, -(k_i - k_o)] \sim \int \frac{d^d q}{(2\pi)^d} \epsilon_{i\mu}\epsilon_{o\nu}^* \frac{q^\mu q^\nu}{D_2 D_3}. \quad (2.13)$$

This integration over  $q$  is non-doable, due to the scalar product of  $q$  and the polarization vector  $\epsilon_{i,o}$  in the numerator. To address this issue, we perform tensor decompositions of the loop integral,

$$\int \frac{d^d q}{(2\pi)^d} \frac{q^\mu q^\nu}{D_2 D_3} = - \int \frac{d^d q}{(2\pi)^d} \frac{k_i^\mu k_o^\nu}{D_2 D_3} - \int \frac{d^d q}{(2\pi)^d} \frac{k_i^\nu k_o^\mu}{D_2 D_3}. \quad (2.14)$$

This is just a simple example of tensor decompositions. Because the number of terms involving  $\epsilon \cdot q$  in the loop integrals is large, many of which are quite complicated, such as  $\frac{\epsilon \cdot q \epsilon^* \cdot q}{D_1 D_2 D_3 D_4}$ , the tensor decomposition is extremely tedious. We use FeynCalc [30, 31] to do this work.

After the tensor decomposition, we can proceed with the calculation of loop integrals. In contrast to the traditional Feynman diagram techniques used in [14] and the on-shell techniques employed in [21], we choose to perform IBP reduction on the loop integrals. Consider the following integral, where  $\mathcal{I}$  is a general scalar integrand,

$$I = \int \prod_{i=1}^L d^d q_i \mathcal{I}. \quad (2.15)$$

Performing an infinitesimal transformation on the loop momentum  $q_i^\mu \rightarrow q_i^\mu + a_{ij} p_j^\mu$ , we obtain

$$\int \prod_{i=1}^L d^d q_i \mathcal{I} \rightarrow \int \prod_{i=1}^L d^d q_i \left( 1 + a_{ij} \frac{\partial p_j^\mu}{\partial q_i^\mu} \right) \left( 1 + a_{ij} p_j^\mu \frac{\partial}{\partial q_i^\mu} \right) \mathcal{I}, \quad (2.16)$$

where  $p_j^\mu \in \{q_1, \dots, q_L, k_1, \dots, k_{n+1}\}$ ,  $k$  represents the external momentum. In dimensional regularization, the above transformation does not change the result of the integral, so we will obtain

$$0 = \int \prod_{i=1}^L d^d q_i a_{ij} \frac{\partial}{\partial q_i^\mu} (p_j^\mu \mathcal{I}). \quad (2.17)$$

Since the integral of eq.(2.15) is a scalar, it is invariant under the Lorentz transformation,

$$I \rightarrow I(k_1 + \delta k_1, \dots) = \left( 1 + \sum_i \omega_\nu^\mu k_i^\nu \frac{\partial}{\partial k^\mu} \right) I, \quad (2.18)$$

which means that,

$$\left( \sum_i \omega_\nu^\mu p_{i,\text{ext}}^\nu \frac{\partial}{\partial k^\mu} \right) I = 0. \quad (2.19)$$

By exchanging the indices  $\mu$  and  $\nu$ , and applying  $\omega_\nu^\mu = -\omega_\mu^\nu$ , we will obtain,

$$\sum_i \left( p_{i,\text{ext}}^\nu \frac{\partial}{\partial k^\mu} - p_{i,\text{ext}}^\mu \frac{\partial}{\partial k^\nu} \right) I = 0. \quad (2.20)$$

Using relations between the Feynman integrals provided by eq.(2.17) and eq.(2.20), we can express the integral  $I$  as a linear combination of simpler scalar integrals

$$I = \sum_i c_i I_i, \quad (2.21)$$

where  $c_i$  refers to coefficients depending on the Lorentz invariants,  $I_i$  is integrals that cannot be simplified further through IBP reduction, i.e. the master integrals. There are many packages available to perform the IBP reduction of Feynman integrals. In this work, we choose LiteRed.

We take the Lorentz invariants in eq.(2.12) as a basis, expressing scalar products of external and loop momentums as linear combinations of this basis, for example

$$k_i \cdot q = -\frac{D_2 - D_1}{2}, \quad p_i \cdot q = \frac{D_4 - D_1}{2}, \quad \dots \quad (2.22)$$

For conveniences, we will use the following notation to denote a general Feynman integration

$$I_{[n_1, n_2, n_3, n_4]} = \int \frac{d^d q}{(2\pi)^d} \frac{1}{D_1^{n_1} D_2^{n_2} D_3^{n_3} D_4^{n_4}}. \quad (2.23)$$

As an example to demonstrate the application of IBP reduction techniques in the calculation of loop integrals, consider the following integral,

$$\int \frac{d^d q}{(2\pi)^d} \frac{k_i \cdot q \, p_i \cdot q}{D_1 D_2 D_3 D_4} = -\frac{1}{4} \int \frac{d^d q}{(2\pi)^d} \frac{D_2 D_4 + D_1^2 - D_1 D_2 - D_1 D_4}{D_1 D_2 D_3 D_4} \quad (2.24)$$

$$\equiv -\frac{1}{4} (I_{[1,0,1,0]} + I_{[-1,1,1,1]} - I_{[0,0,1,1]} - I_{[0,1,1,0]}) \quad (2.25)$$

$$= -\frac{1}{4} \left[ I_{[1,0,1,0]} + \frac{I_{[0,1,0,1]} (m^4 \epsilon - 2m^2 s \epsilon + s^2 \epsilon + st)}{\epsilon (m^2 - s)^2} - \frac{t(\epsilon - 1)(m^2 + s) I_{[0,0,0,1]}}{2m^2 \epsilon (2\epsilon - 1)(m^2 - s)^2} - \frac{(\epsilon - 1)}{m^2 (2\epsilon - 1)} I_{[0,0,0,1]} - 0 \right], \quad (2.26)$$

where the spacetime dimension is set  $d = 4 - 2\epsilon$ . After this operation, the integral we intend to compute, eq.(2.24), is transformed into three simpler scalar integrals  $I_{[0,0,0,1]}$ ,  $I_{[1,0,1,0]}$ ,  $I_{[0,1,0,1]}$  as shown in eq.(2.26). It should be noted that the subdiagram (10) in Figure 3 is a u-topology, while the other diagrams are s-topologies. The basis for these two types of diagrams are different. For the former, the basis is  $D_1, D_2, D_3, D_5$ . While for the latter, it is  $D_1, D_2, D_3, D_4$ . The subdiagram (10) should be reduced separately.



After the IBP reduction, all the loop integrals will be expressed as linear combinations of the following four master integrals,

$$I_{[1,0,1,0]} \equiv \int \frac{d^d q}{(2\pi)^d} \frac{1}{D_1 D_3} \quad (2.27)$$

$$\simeq \frac{i}{16\pi^2} \left[ \frac{1}{\epsilon} + 2 + \log \frac{-\mu^2}{t} + \epsilon \left( \frac{1}{2} \log^2 \frac{-\mu^2}{t} + 2 \log \frac{-\mu^2}{t} + 4 \right) \right],$$

$$I_{[1,0,1,1]} \equiv \int \frac{d^d q}{(2\pi)^d} \frac{1}{D_1 D_3 D_4} \simeq \frac{i}{32\pi^2 m^2} \left[ -\frac{\pi^2 m}{\sqrt{-t}} + \log \frac{-m^2}{t} \right], \quad (2.28)$$

$$I_{[1,1,1,1]}^{(s)} \equiv \int \frac{d^d q}{(2\pi)^d} \frac{1}{D_1 D_2 D_3 D_4} \quad (2.29)$$

$$\simeq \frac{i}{16\pi^2} \left\{ -\frac{2}{t(m^2-s)} \left[ \frac{\log\left(\frac{\mu^2}{m^2}\right)}{\epsilon} + \frac{1}{2} \log^2\left(\frac{\mu^2}{m^2}\right) + \frac{1}{\epsilon^2} \right] + \left[ -\frac{2 \log\left(\frac{m^2}{m^2-s}\right)}{t(m^2-s)} - \frac{\log\left(-\frac{m^2}{t}\right)}{t(m^2-s)} \right] \left[ \log\left(\frac{\mu^2}{m^2}\right) + \frac{1}{\epsilon} \right] + \frac{2\pi^2}{3t(m^2-s)} - \frac{2 \log\left(\frac{m^2}{m^2-s}\right) \log\left(-\frac{m^2}{t}\right)}{t(m^2-s)} \right\},$$

$$I_{[1,1,1,1]}^{(u)} \equiv \int \frac{d^d q}{(2\pi)^d} \frac{1}{D_1 D_2 D_3 D_5} \quad (2.30)$$

$$\simeq \frac{i}{16\pi^2} \left\{ \frac{2}{t(u-m^2)} \left[ \frac{\log\left(\frac{\mu^2}{m^2}\right)}{\epsilon} + \frac{1}{2} \log^2\left(\frac{\mu^2}{m^2}\right) + \frac{1}{\epsilon^2} \right] + \left[ \frac{\log\left(-\frac{m^2}{t}\right)}{t(u-m^2)} + \frac{2 \log\left(\frac{-m^2}{u-m^2}\right)}{t(u-m^2)} \right] \left[ \log\left(\frac{\mu^2}{m^2}\right) + \frac{1}{\epsilon} \right] - \frac{2\pi^2}{3t(u-m^2)} + \frac{2 \log\left(-\frac{m^2}{t}\right) \log\left(\frac{-m^2}{u-m^2}\right)}{t(u-m^2)} \right\}.$$

Expressions of these master integrals can be found in [32], or computed using Package-X [33]. With these expressions, we can write down the complete one-loop amplitude. But this is not the end, we need further finding the corrections to the long-range effective potential between the photon and black holes. Such correction decays as  $r^{-n}$ . Potentials with this behaviour arise from the non-analytic terms in  $t$  within the one-loop amplitude,

$$\mathcal{M}_{\text{non-ana}}(t) = C_1 \log\left(-\frac{\bar{\mu}^2}{t}\right) + C_2 \log\left(-\frac{m^2}{t}\right) + C_3 \sqrt{-\frac{1}{t}} + C_4 \log^2\left(-\frac{\bar{\mu}^2}{t}\right) \quad (2.31)$$

In fact, there are six master integrals appear in the diagram amplitude. But the non-analytic terms happens only in eqs.(2.27)-(2.30). They do not happen in other master integrals that contribute to eq.(2.31). Therefore, we only need computing the four master integrals that include these non-analytic terms in  $t$ , neglecting the contributions from  $I_{[0,0,0,1]}$  and  $I_{[0,1,0,1]}$ .

The low-energy approximation implies that  $\xi \ll \zeta \ll 1$ . Considering this fact, we perform a double series expansion of the one-loop amplitude after the loop integration. Since only the non-analytic terms in  $t$  are relevant, the expansion in  $\xi$  will

be retained up to  $\mathcal{O}(\xi^0)$ , while the expansion in  $\zeta$  will be kept up to  $\mathcal{O}(\zeta^3)$ . The detailed expression is tedious but still readable,

$$\begin{aligned}
i\mathcal{M}_{1\text{-loop}} = i\kappa^4 \left\{ -\frac{m\omega^3}{4608\pi^2} \sin^2 \theta \left[ 18 \log\left(\frac{q^2}{m^2}\right) + 36 \log\left(-\frac{m}{\omega}\right) - 36 \log\left(\frac{m}{\omega}\right) + \right. \right. & (2.32) \\
21 \log\left(\frac{q^2}{\mu^2}\right) - 38 \left. \right] + \frac{m^2\omega^2}{307200\pi^2} \left[ -25 \cos(2\theta) \left\{ 3 \log\left(\frac{q^2}{m^2}\right) \left[ 8 \log\left(\frac{\mu^2}{m^2}\right) + \right. \right. \right. & \\
16 \log\left(\frac{m}{2\omega}\right) + 13 \left. \right] - 48 \log\left(\frac{m}{2\omega}\right) \log\left(\frac{\mu^2}{m^2}\right) - 24 \log^2\left(\frac{\mu^2}{m^2}\right) - 96 \log\left(\frac{\mu^2}{m^2}\right) & \\
-48 \log\left(-\frac{m}{2\omega}\right) - 48 \log\left(\frac{m}{2\omega}\right) + 12 \log^2\left(\frac{q^2}{\mu^2}\right) - 82 \log\left(\frac{q^2}{\mu^2}\right) + 16\pi^2 - 129 \left. \right\} + & \\
4 \cos(\theta) \left\{ 75 \log\left(\frac{q^2}{m^2}\right) \left[ 24 \log\left(\frac{\mu^2}{m^2}\right) + 48 \log\left(\frac{m}{2\omega}\right) - 1 \right] - 3600 \log\left(\frac{m}{2\omega}\right) \log\left(\frac{\mu^2}{m^2}\right) \right. & \\
- 1800 \log^2\left(\frac{\mu^2}{m^2}\right) + 1200 \log\left(\frac{\mu^2}{m^2}\right) + 900 \log^2\left(\frac{q^2}{\mu^2}\right) + 1005 \log\left(\frac{q^2}{\mu^2}\right) + & \\
1200\pi^2 - 2627 \left. \right\} + 15600 \log\left(\frac{q^2}{m^2}\right) \log\left(\frac{m}{2\omega}\right) + 7800 \log\left(\frac{q^2}{m^2}\right) \log\left(\frac{\mu^2}{m^2}\right) + & \\
675 \log\left(\frac{q^2}{m^2}\right) - 15600 \log\left(\frac{m}{2\omega}\right) \log\left(\frac{\mu^2}{m^2}\right) - 7800 \log^2\left(\frac{\mu^2}{m^2}\right) + 2400 \log\left(\frac{\mu^2}{m^2}\right) & \\
- 1200 \log\left(-\frac{m}{2\omega}\right) - 1200 \log\left(\frac{m}{2\omega}\right) + 3900 \log^2\left(\frac{q^2}{\mu^2}\right) + 16370 \log\left(\frac{q^2}{\mu^2}\right) + & \\
5200\pi^2 - 49733 \left. \right] - \frac{m^2\omega^3 \sin^2(\theta)}{256 \sqrt{q^2}} - \frac{m^3\omega}{512\pi^2} \sin^2(\theta) \left[ \log\left(-\frac{m}{2\omega}\right) - \log\left(\frac{m}{2\omega}\right) \right] & \\
+ \frac{m^3\omega^2}{1024} \frac{3 \cos^2\left(\frac{\theta}{2}\right) (\cos(\theta) + 9)}{\sqrt{q^2}} & \\
- \frac{m^3\omega^3}{16\pi^2 t} \cos^2\left(\frac{\theta}{2}\right) \left[ \log\left(-\frac{m}{2\omega}\right) - \log\left(\frac{m}{2\omega}\right) \right] \left[ \log\left(\frac{q^2}{m^2}\right) - \log\left(\frac{\mu^2}{m^2}\right) \right] \left. \right\}. &
\end{aligned}$$

In the small-angle approximation, we sum the tree-level amplitude in eq.(2.10) with the one-loop amplitude in eq.(2.32). Keeping terms up to  $\mathcal{O}(\theta^0)$ , and applying eq.(2.7), we will obtain

$$\begin{aligned}
i\mathcal{M}_{1\text{-loop}}^{\theta^0} = \frac{\kappa^2 m^2 \omega^2}{\mathbf{q}^2} + \frac{15\kappa^4 m^3 \omega^2}{512\sqrt{\mathbf{q}^2}} + \frac{3\kappa^4 m^2 \omega^2}{128\pi^2} \log^2\left(\frac{\mathbf{q}^2}{\bar{\mu}^2}\right) - \frac{\mathcal{B}\kappa^4 m^2 \omega^2}{(8\pi)^2} \log\left(\frac{\mathbf{q}^2}{\bar{\mu}^2}\right) & \\
+ \log\left(\frac{\mathbf{q}^2}{m^2}\right) \left[ -\frac{\kappa^4 m^2 \omega^2}{512\pi^2} + \frac{3\kappa^4 m^2 \omega^2}{64\pi^2} \log\left(\frac{\bar{\mu}^2}{4\omega^2}\right) \right]. & (2.33)
\end{aligned}$$

Careful algebra yields  $\mathcal{B} = \frac{103}{40}$ .

### 3 The deflection angle of photon trajectory

In this section, we provide the detailed operation to get the deflection angle of the photon trajectory from eq.(2.33).

### 3.1 Geometric optics approximation

Since the wavelength  $\lambda$  of the photon is much smaller than the horizon scale  $2G_N m$  of the black hole, we can describe the propagation of photons using geometric optics. According to ref.[34], this is controlled by

$$\frac{d}{ds} \left( n \frac{d\mathbf{r}}{ds} \right) = \nabla n, \quad (3.1)$$

where  $\mathbf{r}$  is the position vector of the photon,  $s$  is the affine parameter along its path, and  $n$  is the refractive index. We will choose the coordinate time  $t$  as the affine parameter for the photon, so that the above equation becomes:

$$\frac{1}{c^2} \frac{d^2 \mathbf{r}}{dt^2} = \frac{1}{n} \nabla n. \quad (3.2)$$

The gravitational field deflecting our photon trajectories is that of the standard Schwarzschild black holes

$$ds^2 = -h(r)dt^2 + h^{-1}(r)dr^2 + r^2(d\theta^2 + \sin^2 \theta d\varphi^2), \quad (3.3)$$

$$h = 1 - \frac{2G_N m}{r}. \quad (3.4)$$

According to [35], in a spacetime described by the Schwarzschild metric (3.3), the refractive index of (3.2) can be written in the following form,

$$n = \sqrt{\frac{1}{h^2}} = \frac{1}{1 - \frac{2G_N m}{r}} \simeq 1 - V_{\text{eff}}(r). \quad (3.5)$$

By a Fourier transformation of (2.33), we can obtain the effective potential  $\omega \cdot V_{\text{eff}}$  of the photon-black hole interaction. From eq.(3.5), we know that in the region  $r \gg 2G_N m$ ,  $n$  can be expressed as functions of the effective gravitational potential,

$$\begin{aligned} \omega V_{\text{eff}}(r) = & -\frac{2G_N m \omega}{r} - \frac{15G_N^2 m^2 \omega}{4r^2} + \frac{2G_N^2 \mathcal{B} m \omega}{\pi r^3} - \frac{G_N^2 m \omega}{4\pi r^3} \\ & - \frac{12G_N^2 m \omega}{\pi r^3} \log \frac{r}{b_0} + \frac{6G_N^2 m \omega}{\pi r^3} \log \frac{\bar{\mu}^2}{4\omega^2}. \end{aligned} \quad (3.6)$$

Substituting eqs.(3.5)&(3.6) into (3.2), and performing the integration over  $t$ , we will get

$$\frac{1}{c^2} \frac{d\mathbf{r}}{dt} = -\frac{1}{\omega} \int dt \nabla(\omega V_{\text{eff}}). \quad (3.7)$$

In the absence of gravitational potentials, the position vector of the photon can be approximately written as  $\mathbf{r} = b\hat{\mathbf{x}} + ct\hat{\mathbf{z}}$ , as shown in Figure 4. The deflection angle of the photon's outgoing momentum  $\vec{k}_{\text{out}}$  relative to the incoming momentum  $\vec{k}_{\text{in}}$  is

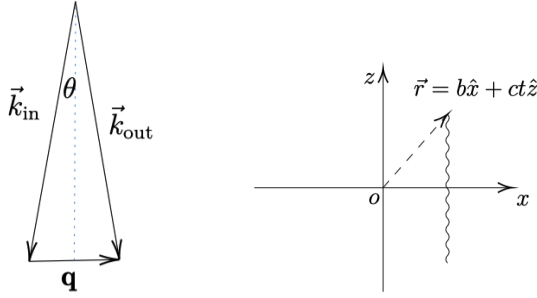


**Figure 4.** left:small angle approximation, right:the trajectory of photon without the potential. The wavy line in the right panel is the photon trajectory and  $b$  is the impact parameter relative to the central black holes.

very small, as shown in left panel of Figure 4. Similarly, the deflection angle  $\theta$  of the photon's position vectors  $\mathbf{r}_{\text{in}}$  and  $\mathbf{r}_{\text{out}}$  is also small. Therefore,

$$\frac{1}{c} \sin \frac{\theta}{2} = - \int dt \nabla V_{\text{eff}}(r) \Rightarrow \theta \simeq - \int dt V'_{\text{eff}}(\sqrt{b^2 + c^2 t^2}) \frac{b}{\sqrt{b^2 + c^2 t^2}}. \quad (3.8)$$

Let  $t = \frac{bu}{c}$ , we can easily show that

$$\theta = -b \int_{-\infty}^{+\infty} du V'_{\text{eff}}(b\sqrt{1+u^2}) \frac{1}{\sqrt{1+u^2}} \quad (3.9)$$

$$= \frac{4G_N m}{b} + \frac{15\pi G_N^2 m^2}{4b^2} + \frac{G_N^2 m \hbar}{\pi b^3} \left( 8\mathcal{B} + 9 + 16 + 48 \log \frac{b}{2b_0} + 24 \log \frac{\bar{\mu}^2}{4\omega^2} \right). \quad (3.10)$$

This is our deflection angle of photons derived from the geometric optics approximation, where  $\bar{\mu}^2 = 4\pi e^{-\gamma_E} \mu^2$ , while  $b_0^{-1} = e^{1-\gamma_E} \bar{\mu}$  is the infrared cutoff mass.

### 3.2 Eikonal approximation

Before applying the Eikonal approximation, we need to point out a key feature of the transferred momentum  $q^\mu$ . According to the on-shell condition for the external photon, we have

$$k_i \cdot k_i = k_o \cdot k_o = 0. \quad (3.11)$$

If we assume that  $q^\mu$  has a non-zero component in the  $z$ -direction, then the outgoing photon momentum can be written as  $k_o^\mu = (\omega, q_x, q_y, \omega + q_z)$ . In this case, taking the square of the modulus of  $k_o^\mu$  and applying eq.(3.11), we will have

$$0 = \omega^2 - q_x^2 - q_y^2 - (\omega + q_z)^2 = q_x^2 + q_y^2 + q_z^2 - 2\omega \cdot q_z \Rightarrow \quad (3.12)$$

$$\mathbf{q}^2 = 2\mathbf{k}_i \cdot \mathbf{q}, |\mathbf{q}| = 2\mathbf{k}_i \cdot \hat{\mathbf{q}} = 2\omega \cos \theta. \quad (3.13)$$

The low-energy approximation requires  $|\mathbf{q}| \ll \omega$ , which implies that  $\cos \theta \ll 1$  according to eq.(3.13). Since  $\mathbf{k}_i$  has only a component along the  $z$ -axis, eq.(3.13) shows

that  $\mathbf{q}$  has almost no component along  $\mathbf{k}_i$ , the momentum of the ingoing photon. In another word, the transferred momentum of the scattering is dominated by the transverse component. According to [21, 36], we can write the scattering amplitude in the collisional space as

$$\tilde{\mathcal{M}}(\mathbf{b}) = \int \frac{d^2\mathbf{q}}{(2\pi)^2} \mathcal{M}(\mathbf{q}) e^{-i\mathbf{q}\cdot\mathbf{b}}. \quad (3.14)$$

Applying the eikonal approximation, this expression can be written in the following form,

$$i\tilde{\mathcal{M}}(\mathbf{b}) \simeq 2(s - m^2) \{ \exp [i\tilde{M}_t(\mathbf{b}) + i\tilde{M}_{1\text{-loop}}(\mathbf{b})] - 1 \}, \quad (3.15)$$

where

$$\tilde{M}_t(\mathbf{b}) = \frac{1}{4m\omega} \int \frac{d^2\mathbf{q}}{(2\pi)^2} \mathcal{M}_t(\mathbf{q}) e^{i\mathbf{q}\cdot\mathbf{b}}, \quad (3.16)$$

$$\tilde{M}_{1\text{-loop}}(\mathbf{b}) = \frac{1}{4m\omega} \int \frac{d^2\mathbf{q}}{(2\pi)^2} \mathcal{M}_{1\text{-loop}}(\mathbf{q}) e^{i\mathbf{q}\cdot\mathbf{b}}. \quad (3.17)$$

According to [36], we can calculate the scattering angle by the stationary phase approximation. Considering the calculation of scattering amplitude in the transferred momentum space

$$\int d^2\mathbf{b} i\mathcal{M}(\mathbf{b}) e^{-i\mathbf{q}\cdot\mathbf{b}} = \int d^2\mathbf{b} \left\{ 2(s - m^2) \left( \exp [i\tilde{M}_t(\mathbf{b}) + i\tilde{M}_{1\text{-loop}}(\mathbf{b})] - 1 \right) \right\} e^{-i\mathbf{q}\cdot\mathbf{b}}, \quad (3.18)$$

the stationary phase approximation says that the main contribution of the right-hand integration comes from the region around  $\frac{\partial \text{phase}}{\partial b} = 0$ ,

$$0 = \frac{\partial}{\partial b} \left[ -\mathbf{q} \cdot \mathbf{b} + \tilde{M}_t(\mathbf{b}) + \tilde{M}_{1\text{-loop}}(\mathbf{b}) \right] = 2\omega \sin \frac{\theta}{2} + \frac{\partial \tilde{M}_t(\mathbf{b})}{\partial b} + \frac{\partial \tilde{M}_{1\text{-loop}}(\mathbf{b})}{\partial b} \quad (3.19)$$

According to Figure 4, we can express  $q$  in (3.19) as  $2\omega \sin \frac{\theta}{2}$ . Performing the series expansion of eqs.(2.10) and (2.32) up to  $\mathcal{O}(\theta^0)$ , translating into impact parameter space with eqs.(3.16)-(3.17) and substituting the resultant amplitude into eq.(3.19), we will obtain

$$\theta \simeq -\frac{1}{\omega} \left[ \frac{\partial \tilde{M}_t^{\theta^0}(\mathbf{b})}{\partial b} + \frac{\partial \tilde{M}_{1\text{-loop}}^{\theta^0}(\mathbf{b})}{\partial b} \right] \quad (3.20)$$

$$= \frac{4G_N m}{b} + \frac{15\pi G_N^2 m^2}{4b^2} + \frac{G_N^2 m \hbar}{\pi b^3} \left( 8\mathcal{B} + 9 + 16 + 48 \log \frac{b}{2b_0} - 24 \log \frac{\bar{\mu}^2}{4\omega^2} \right). \quad (3.21)$$

This is our deflection angle of photons derived from the Eikonal approximation.

### 3.3 Discussion on the result

This section is devoted to comparing our deflection angle expressions in eqs.(3.10) and (3.21) with those in the literatures. On the classic part, our result can be compared with those derived in classical general relativity and Gauss-Bonnet topological method [5, 37],[6, 10]

$$\theta_{\text{GR}} \simeq \frac{4G_N m}{b} + \frac{4G_N^2 m^2}{b^2} \left( \frac{15\pi}{16} - 1 \right) + \mathcal{O} \left( \frac{G_N^3 m^3}{b^3} \right), \quad (3.22)$$

$$\theta_{\text{GB}} \simeq \frac{4G_N m}{b} + \frac{3\pi G_N^2 m^2}{4b^2}. \quad (3.23)$$

Obviously, at the leading order, our result is consistent with those from classic GR and GB topological method. At the next leading order, our result is nearly twice as large as that from GR and five times as large as that from GB-topological method. Nevertheless, the classic part of our result matches with those from references [14, 16, 21], which calculate the deflection angle with EFT method. Results basing on EFT contain quantum corrections which arises from the quantum feature of gravitational interactions between the photon and black holes, rather than the quantum-effect-modified spacetime geometry [10, 38].

However, the quantum part in our results (3.10) and (3.21) does not match those of references [14, 16, 21] bit by bit. The differences are as follows.

1. The coefficient structure of the non-log part of our results ( $8\mathcal{B} + 9 + 16$ ), is the same as in that of [16]. However, we note that different works yield different values for parameter  $\mathcal{B}$ . For example, our calculation yields  $\mathcal{B} = \frac{103}{40}$ ; ref.[14] yeilds  $\mathcal{B} = \frac{113}{120}$ ; ref.[16](scalar photon) yeilds  $\mathcal{B} = -\frac{3}{40}$ ; even the same literature [21], different values are obtained for the scattering of different particle types, scalar  $\mathcal{B} = \frac{3}{40}$ , spinor  $\mathcal{B} = -\frac{31}{30}$ , while vector  $\mathcal{B} = -\frac{161}{120}$ . Although equivalence principle requires that these parameters be universal, ref.[21] argues that the incomplete series of EFT has no reason to capture the full geometric feature of general relativity. We do not understand the origin of the discrepancy among different works.
2. The coefficient of the  $\log \frac{b}{2b_0}$  term: the expression of [16] based on geometric optics approximation differs by a negative sign from that based on eikonal approximation, but those of [21] are the same. Our expressions based on the two methods show no sign difference, but differ from those of [21] by a negative sign. The is because we used the following Fourier transformation formula

$$\int \frac{d^2 \mathbf{q}}{(2\pi)^3} e^{-i\mathbf{q}\cdot\mathbf{r}} \log^2 \mathbf{q}^2 = \frac{4}{\pi r^2} + \frac{4}{\pi r^2} \log \frac{r}{2r_0}, \quad (3.24)$$

where  $r_0 = e^{1-\gamma_E}$ . While the transformation formula of [16, 21] reads as follows

$$\int \frac{d^2\mathbf{q}}{(2\pi)^3} e^{-i\mathbf{q}\cdot\mathbf{r}} \log^2 \mathbf{q}^2 = \frac{4}{\pi r^2} \log \frac{2}{r}. \quad (3.25)$$

By (3.24) the contribution of  $\log^2 \frac{\bar{\mu}^2}{\mu^2}$  to the long-range potential  $V_{\text{eff}}$  is attractive. While by (3.25), such a contribution will be repellent.

3. The  $\log \frac{\bar{\mu}^2}{4\omega^2}$  term appears in [16], but not in [14, 21]. The reason is that [14, 21] used the monodromy BCJ relation,

$$\frac{C_s}{m^2 - s} + \frac{C_u}{m^2 - u} = \text{Coefficient of } I_{[1,1,1,0]}, \quad (3.26)$$

where  $C_{s/u}$  is the coefficient of the  $I_{1,1,1,1}^{(s/u)}$  integration. By this relation in the low-energy limit, the loop amplitude can be expressed into the following form

$$i\mathcal{M}_X^{(2)} \simeq \frac{\mathcal{N}^X}{\hbar} \left[ \hbar \frac{\kappa^4}{4} (4(M\omega)^4 (I_4(t, u) + I_4(t, s)) + 3(M\omega)^2 t I_3(t) - 15 (M^2\omega)^2 I_3(t, M) + bu^X (M\omega)^2 I_2(t)) \right], \quad (3.27)$$

where

$$I_4(t, u) + I_4(t, s) \simeq \frac{4\pi}{2tm\omega} \log \left[ -\frac{t}{m^2} \right]. \quad (3.28)$$

$$I_3(t, M) = I_{[1,0,1,1]}, \quad I_3(t) = I_{[1,1,1,0]}, \quad I_2(t) = I_{[1,0,1,0]}$$

It is the use of eqs.(3.26)&(3.28) that leads to the absence of  $\log \frac{\bar{\mu}^2}{4\omega^2}$ -proportional terms from the expressions of [14, 21].

## 4 Conclusion

By the effective field theory method and in the weak-field limit, we calculated the one-loop scattering amplitude of an electromagnetic field off a heavy scalar field through gravitational interactions. The relevant Feynman diagrams are presented in Figure 3. To simplify the computation, we employed Integration-By-Parts (IBP) reduction techniques, which reduced the problem to four master integrals, significantly decreasing the complexity of the loop integral evaluations. Focusing on small deflection angles, we isolated the contribution from long-range gravitational interactions by retaining terms in the scattering amplitude up to  $\mathcal{O}(t^0, \omega^3, \theta^0)$ . Utilizing geometric optics and eikonal approximations, we derived the photon deflection angle caused by a massive celestial object and compared our results with those reported in the existing literature.

Unlike traditional QFT approach, we only applied the non-analytic terms in  $t$  of the scattering amplitude to extract the deflection angle  $\theta$ . To ensure the covariance of the EFT Lagrangian, we adopted  $\frac{(D_\mu A^\mu)^2}{2}$  as the gauge fixing term for the electromagnetic field and imposed the harmonic coordinate condition as gauge fixing condition for the gravitational field. Our calculation incorporates contributions from the scalar and vector ghost fields to the scattering amplitude. The resulting expressions of the deflection angle are compared with those reported in existing literatures. Discrepancies are explicitly identified, and their underlying origins are analyzed in detail.

Our work serves as a supplement to the calculation of light deflection angles in the weak gravitational field. The methods employed here are limited to the low-energy regime ( $b \gg 2G_N m, t \ll \omega^2 \ll m^2$ ) and are not applicable to scenarios involving strong gravitational fields. For such cases, alternative approaches, such as those developed by V. Bozza and N. Tsukamoto, should be utilized. Additionally, we acknowledge that the EFT method may not be the optimal choice for obtaining higher-order correction terms. This limitation arises because, as the perturbative order increases, the complexity of the calculations grows significantly. Specifically, the number and variety of graviton-matter interaction and graviton-graviton self-interaction vertices increase dramatically. Notably, the appearance of four-graviton self-coupling vertices introduces expressions of considerable complexity, which makes the EFT approach less practical for such computations.

## References

- [1] Event Horizon Telescope Collaboration et.al. First m87 event horizon telescope results. iv. imaging the central supermassive black hole. *The Astrophysical Journal Letters*, 875(1):L4, April 2019.
- [2] Kazunori Akiyama, Antxon Alberdi, and et.al. First m87 event horizon telescope results. v. physical origin of the asymmetric ring. *The Astrophysical Journal Letters*, 875(1):L5, April 2019.
- [3] Event Horizon Telescope Collaboration et al. First m87 event horizon telescope results. ii. array and instrumentation. *The Astrophysical Journal Letters*, 875(1):L2, April 2019.
- [4] Event Horizon Telescope Collaboration et al. First sagittarius a\* event horizon telescope results. i. the shadow of the supermassive black hole in the center of the milky way. *The Astrophysical Journal Letters*, 930(2):L12, May 2022.
- [5] K. S. Virbhadra and George F. R. Ellis. Schwarzschild black hole lensing. *Physical Review D*, 62(8), September 2000.
- [6] G W Gibbons and M C Werner. Applications of the gauss–bonnet theorem to



- gravitational lensing. *Classical and Quantum Gravity*, 25(23):235009, November 2008.
- [7] Simonetta Frittelli, Thomas P. Kling, and Ezra T. Newman. Spacetime perspective of schwarzschild lensing. *Phys. Rev. D*, 61:064021, Feb 2000.
- [8] V. Bozza, S. Capozziello, G. Iovane, and G. Scarpetta. Strong field limit of black hole gravitational lensing. *General Relativity and Gravitation*, 33(9):1535–1548, 2001.
- [9] Naoki Tsukamoto. Deflection angle in the strong deflection limit in a general asymptotically flat, static, spherically symmetric spacetime. *Physical Review D*, 95(6), March 2017.
- [10] N. Heidari, A. A. Araújo Filho, R. C. Pantig, and A. Övgün. Absorption, scattering, geodesics, shadows and lensing phenomena of black holes in effective quantum gravity, 2024.
- [11] John F. Donoghue. General relativity as an effective field theory: The leading quantum corrections. *Physical Review D*, 50(6):3874–3888, September 1994.
- [12] John F. Donoghue. Leading quantum correction to the newtonian potential. *Physical Review Letters*, 72(19):2996–2999, May 1994.
- [13] John F. Donoghue and Tibor Torma. Infrared behavior of graviton-graviton scattering. *Physical Review D*, 60(2), June 1999.
- [14] Dong Bai and Yue Huang. More on the bending of light in quantum gravity. *Phys. Rev. D*, 95:064045, Mar 2017.
- [15] E. Guadagnini. Gravitational deflection of light and helicity asymmetry. *Physics Letters B*, 548(1):19–23, 2002.
- [16] Giacomo Brunello. Effective field theory approach to general relativity and feynman diagrams for coalescing binary systems, 2022.
- [17] Zvi Bern. Perturbative quantum gravity and its relation to gauge theory. *Living Reviews in Relativity*, 5(1), July 2002.
- [18] Z. Bern, J. J. M. Carrasco, and H. Johansson. New relations for gauge-theory amplitudes. *Physical Review D*, 78(8), October 2008.
- [19] Lance J Dixon. A brief introduction to modern amplitude methods, 2014.
- [20] N. E. J. Bjerrum-Bohr, John F. Donoghue, Barry R. Holstein, Ludovic Planté, and Pierre Vanhove. Bending of light in quantum gravity. *Phys. Rev. Lett.*, 114:061301, Feb 2015.
- [21] N. Emil J. Bjerrum-Bohr, John F. Donoghue, Barry R. Holstein, Ludovic Planté, and Pierre Vanhove. Light-like scattering in quantum gravity. *Journal of High Energy Physics*, 2016, 2016.
- [22] Laporta. High-precision calculation of multi-loop feynman integrals by difference equations. *International Journal of Modern Physics A*, 15:5087, 2000.

- [23] Roman Lee. Presenting litered: a tool for the loop integrals reduction. 12 2012.
- [24] Roman N Lee. Litered 1.4: a powerful tool for reduction of multiloop integrals. *Journal of Physics: Conference Series*, 523(1):012059, jun 2014.
- [25] J.M. Martín-García, R. Portugal, and L.R.U. Manssur. The invar tensor package. *Computer Physics Communications*, 177(8):640–648, October 2007.
- [26] J.M. Martín-García, D. Yllanes, and R. Portugal. The invar tensor package: Differential invariants of riemann. *Computer Physics Communications*, 179(8):586–590, October 2008.
- [27] José M. Martín-García. xperm: fast index canonicalization for tensor computer algebra. *Computer Physics Communications*, 179(8):597–603, October 2008.
- [28] B Latosh. Feyngrav: Feyncalc extension for gravity amplitudes. *Classical and Quantum Gravity*, 39(16):165006, July 2022.
- [29] B. Latosh. Feyngrav 2.0. *Computer Physics Communications*, 292:108871, November 2023.
- [30] R. Mertig, M. Böhm, and A. Denner. Feyn calc - computer-algebraic calculation of feynman amplitudes. *Computer Physics Communications*, 64(3):345–359, 1991.
- [31] Vladyslav Shtabovenko, Rolf Mertig, and Frederik Orellana. Feyncalc 9.3: New features and improvements. *Computer Physics Communications*, 256:107478, November 2020.
- [32] Giulia Zanderighi R.Keith Ellis. Scalar one-loop integrals for qcd. *JHEP 02 (2008) 002*, 2008.
- [33] Hiren H. Patel. Package -x 2.0: A mathematica package for the analytic calculation of one-loop integrals. *Computer Physics Communications*, 218:66–70, September 2017.
- [34] Charles A. Brau. Modern problems in classical electrodynamics. 2003.
- [35] Paul M. Alsing. *The optical-mechanical analogy for stationary metrics in general relativity*. Am.J.Phys, 1998.
- [36] Ratindranath Akhoury, Ryo Saotome, and George Sterman. High energy scattering in perturbative quantum gravity at next-to-leading power. *Physical Review D*, 103(6), March 2021.
- [37] K. S. Virbhadra, D. Narasimha, and S. M. Chitre. Role of the scalar field in gravitational lensing, 1998.
- [38] Cong Zhang, Jerzy Lewandowski, Yongge Ma, and Jinsong Yang. Black holes and covariance in effective quantum gravity, 2024.